FACTA UNIVERSITATIS
Series: **Mechanical Engineering** Vol. 2, N° 1, 2004, pp. 69 - 82

APPROXIMATE CONTACT MODELS OF THE ROLLING SUPPORTS [1]

UDC 626.422.4:624.078.54

Miomir Jovanović, Predrag Milić, Danko Mijajlović

Mechanical Faculty University of Niš, Serbia and Montenegro

Abstract. *The paper deals with contact problem in huge rolling supports, used in industry and buildings. One of the main questions is the choice of the analysis type for the carrying elements check. In this paper linear and nonlinear contact static analyses are applied simultaneously. The aim is to identify the approximations and differences in the results on actual examples. The first performed analysis is was numerical, using FEA, based on the classical Hertz concept. Thereby the constraints are unchangeable during the load appliance, while the force is approximated with surface pressure according to the square parabolic law. One approximate procedure for the surface pressure determination is shown. These solutions are compared to the analysis based on the nonlinear contact theory. The nonlinear analysis better defines the stress distribution in the structure, because it uses variable boundary conditions, friction, sliding and the rigidity of bodies in contact. Further, the modeling of the same contact task through two different nonlinear models is shown and the comparison of all the three models is given. The results are given graphically and numerically. The finite element meshes, the model properties and composite stresses in contact zones are shown. The objective evaluation of these analyses gave the support behavior in practice.*

Key Words: *Contact Pairs, FEM, Contact Analysis, Contact Models, Approximative Models*

1. INTRODUCTION

The structural analysis of the biggest rolling supports is an exclusive category with the demand of highest engineering reliability. Therefore, three different approximate models were used, and numerical solutions using Finite Element Method were calculated. The technical solution for the given support [5] was used for the analysis, formed of two flat plates with the rolling body in between. The plates and the rolling body are massive constructive elements of alloy steel[2], Fig. 1. How much engineering solutions of the model

Received December 29, 2003
[1] The paper was realized in the project of Ministry of Science and Environmental Protection of the Republic of Serbia TR3.07.0082
[2] Yield point $\mathbf{R}_H < 560$ MPa and tensile strength $\mathbf{R}_M = 800$ MPa,

can differ is the most important question. This question can be directly answered if a number of analyses are done, first simplified – linear, and afterwards nonlinear ones. Real industrial tasks overreach the complexity of *Hertz's* model because of the bending as an additive influence. Furthermore, plastic deformation can appear in the construction, which inducts sliding of the contact surfaces. The approximation comparison is shown in the following text, through three given models, which differ according to the influence complexity and mechanical models of the analysis. These models are given in the following text.

2. LINEAR ANALYSIS: MODEL-1

The simplest model analysis is a linear one. The classical elasticity finite element method was used, where the structure equation is **[K]•{q}={F}** in which the rigidity matrix does not depend on generalized displacements **{q}** and generalized action **{F}**. The rolling support construction was modeled using 3D solid finite elements, with eight nodes, and linear shape functions with three degrees of freedom at each node.

MODEL-1 (Fig. 1) treated directly the flat element of the support (the thick plate). The finite element mesh was made to have a bigger density in the contact area; besides, it was made according to the theoretical contact surface and the idea to lead in the surface pressure in few (8) discrete stress levels. Fig. 2 shows the discrete model of one half of the support plate. The surface pressure was spread according to the parabolic law in the cross section, Fig. 3. The pressure is uniform along the contact length. At the opposite side of the contact two lines of supports were placed (as appropriate for huge constructions). Thus defined model is obvious and simple. The choice of the comparative stress for the stress level evaluation in the contact was made according to the expectance of elastic behavior, where the greatest amount of the energy is used for geometry deformation, (*Hencky-Huber-Mises* method). Maximal comparative stresses were analyzed and determined in the contact array.

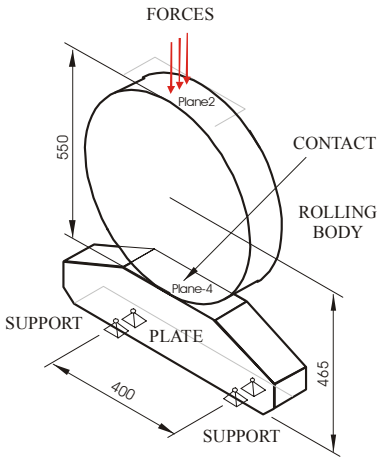

Fig. 1. Rolling Support Geometry in the Linear Analysis

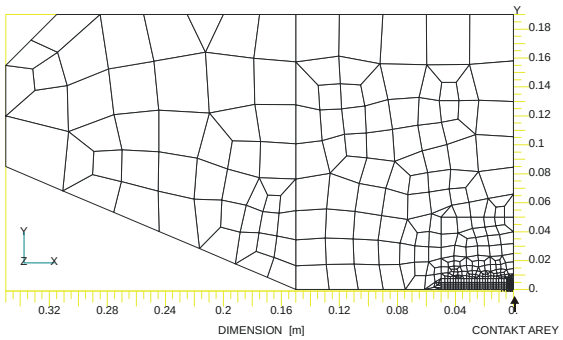

Fig. 2. Support Plate Model (Half Section Topology)

The discrete FEM model was realized on half of the construction, which is possible because of the symmetry in geometry, supports and load. The influence of the rest of the structure was taken into account through boundary conditions. The half of the model treatment in return enabled the increasing of the number of the finite elements in the model. The realized discrete model satisfies the theoretical conditions for the 3D meshes topology development [7, 8]. The mesh was applied uniformly through the region depth. In the lower section of the part the contact area is indicated in Fig. 2.

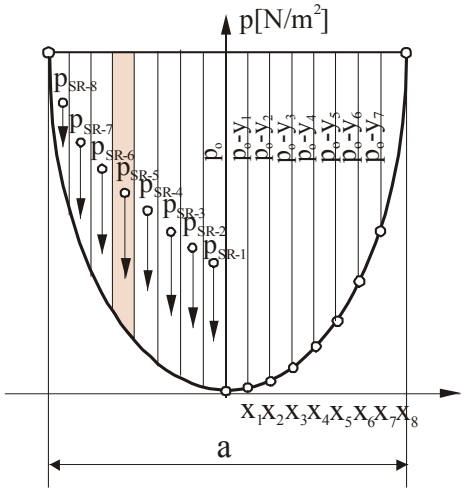

Fig. 3. Parabola of the Pressure

The contact influence of the cylinder is defined through surface loads (surface pressure), as defined in literature [2], and spreads according to the square parabola law in contact between cylinder and endless flat surface (plate). Based on this law for spreading through continuum the surface pressure on the contact surfaces can be defined. In the model treated (MODEL-1) the force $F=6.9\cdot10^6$ [N] was applied onto the whole contact surface. The working force was taken according to the real support from practice [5]. The half of the contact surface was modeled with 8 elements in the cross section of the plate, fig. 2. Based on this, the half of force corresponds to the sum of surface pressures onto the 8 corresponding parts of the pressure parabola. In this way the concentrated working force was applied through discrete changeable surface pressure in 8 stripe-like contact zones. The realization of the approximation demands the determination of the parabola law. This was made according to the contact width and maximal surface pressure. The maximal pressure is calculated from the equality of total surface pressure and given working force in the support. The opening of the parabola (the contact width) **a** is determined according to relation (1), [2]. For that calculation the unit continual load along the length of the whole support is used q=F/L=6900000./0.98=7040816. [N/m']. In this relation, the support length is L=0.98 [m], diameter of the cylinder in contact D=0.55 [m] and module of elasticity of steel applied $E=2.1\ 10^{11}$ [N/m^2] to real object [5]:

$$a = 2.15\sqrt{\frac{q \cdot D}{E}} = 2.15\sqrt{\frac{7040816 \cdot 0.55}{2.1 \cdot 10^{11}}} = 9.2 \cdot 10^{-3} \ [\mathrm{m}] \tag{1}$$

The total impact (contact) was accomplished on the width of 16 equal parabola stripes (Fig. 3), which gives single width of stripe (zone) of parabola: $\Delta x = \mathbf{a}/16 = 0.575 \cdot 10^{-3}$ [m]. Out of this width the coordinates of symmetric parabola half $\mathbf{x}_i$ come out, as showed in the tabular way in T1. Starting from square parabola equation $\mathbf{y = k \cdot x^2}$, with unknown (requested) pressure ordinate p_0, coefficient **k** of the parabola searched will have the value: $\mathbf{k = y_{max}/x^2_8 = p_0/(4.6 \cdot 10^{-3})^2} = 4.7259 \cdot 10^4 \cdot \mathbf{p_0}$. Now, the ordinates are further defined as a function of unknown parameter $\mathbf{p_0}$ and given in T1.

Table T1

Band of parabola No: Fig. 3	1	2	3	4	5	6	7	8
Coordinates x_i [m]	0.000575	0.001150	0.001725	0.002300	0.002875	0.003450	0.004025	0.004600
Coordinates y_i [m]	$0.0156 \cdot p_0$	$0.0625 \cdot p_0$	$0.1406 \cdot p_0$	$0.2500 \cdot p_0$	$0.3906 \cdot p_0$	$0.5625 \cdot p_0$	$0.7656 \cdot p_0$	$1.0000 \cdot p_0$

The individual eight surfaces of the pressure parabola half treated can be evaluated by integration in the extending boundaries. The parabola surfaces along contact length L, correspond to concentrated forces F_i ($i=1 \div 8$) to which the plate is exposed, on the individual widths of contact surfaces, given in relations (2):

$$\begin{aligned}
F_1 &= \Delta x \cdot L \cdot p_0 - L\int_0^{x_1} 4.7259 \cdot 10^4 \cdot p_0 \cdot x^2 \cdot dx = 0.00056056 \cdot p_0, \\
F_2 &= \Delta x \cdot L \cdot p_0 - L\int_{x_1}^{x_2} 4.7259 \cdot 10^4 \cdot p_0 \cdot x^2 \cdot dx = 0.0005429 \cdot p_0, \\
F_3 &= \Delta x \cdot L \cdot p_0 - L\int_{x_2}^{x_3} 4.7259 \cdot 10^4 \cdot p_0 \cdot x^2 \cdot dx = 0.0005077 \cdot p_0, \\
F_4 &= \Delta x \cdot L \cdot p_0 - L\int_{x_3}^{x_4} 4.7259 \cdot 10^4 \cdot p_0 \cdot x^2 \cdot dx = 0.0004549 \cdot p_0, \\
F_5 &= \Delta x \cdot L \cdot p_0 - L\int_{x_4}^{x_5} 4.7259 \cdot 10^4 \cdot p_0 \cdot x^2 \cdot dx = 0.0003845 \cdot p_0, \\
F_6 &= \Delta x \cdot L \cdot p_0 - L\int_{x_5}^{x_6} 4.7259 \cdot 10^4 \cdot p_0 \cdot x^2 \cdot dx = 0.0002965 \cdot p_0, \\
F_7 &= \Delta x \cdot L \cdot p_0 - L\int_{x_6}^{x_7} 4.7259 \cdot 10^4 \cdot p_0 \cdot x^2 \cdot dx = 0.0001908 \cdot p_0, \\
F_8 &= \Delta x \cdot L \cdot p_0 - L\int_{x_7}^{x_8} 4.7259 \cdot 10^4 \cdot p_0 \cdot x^2 \cdot dx = 0.0000676 \cdot p_0,
\end{aligned} \tag{2}$$

The sum of single pressure forces on the left and right side of y-axis gives total pressure force F on the support. From the balance according to equation (3), the requested integration constant – pressure p_0 is found:

$$2 \cdot \sum_{1}^{8} F_i = F$$
$$2 \cdot (0.0005606 + 0.0005429 + 0.0005077 + 0.0004549 + 0.0003845 + 0.0002965 + 0.0001908 + 0.0000676) \cdot p_0 = 6.9 \cdot 10^6 \quad (3)$$
$$p_0 = 6.9 \cdot 10^6 / 0.0060109 = 1.14791 \cdot 10^9 \left[\frac{N}{m^2}\right]$$

The ending points of surface pressures $\mathbf{p_i = p_0 - y_i}$ in stripes 1÷8 are determined from ordinates $\mathbf{y_i}$ in the parabola equation and they are shown in Table T2. The average-middle values of surface pressures p_{SRi+1} (on the contact surfaces) are evaluated out of the discrete pressure values on the endings of stripe contact (zone) surfaces $\mathbf{p_i}$ according to relation (4) and they are given in the tabular form in T2:

$$p_{SRi+1} = \tfrac{1}{2}(p_i + p_{i+1}) \quad [N/m^2], \quad (4)$$

These values are used as uniform pressures in 8 zones treated for the linear analysis, allocated according to the parabola in Fig. 3. In this way the influences on the supporting plate are approximately determined. The solution deducted by the linear analysis of the contact task, using the finite element method, gave compound stresses according to the *Hencky-Huber-Mises* hypothesis, along with the tangent stresses, in the contact zone, showed in Figs. 4, 5.

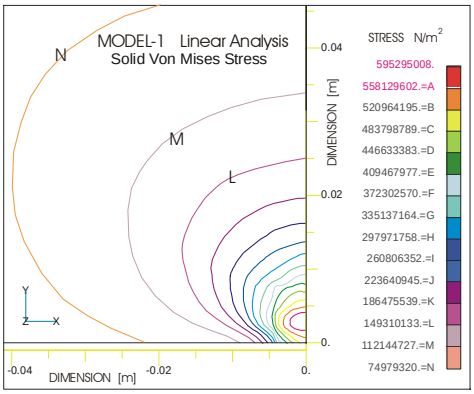

Fig. 4. Iso Lines for Compound Stresses According to the *Hencky-Huber-Mises* Hypothesis in Linear Analysis (MODEL-1)

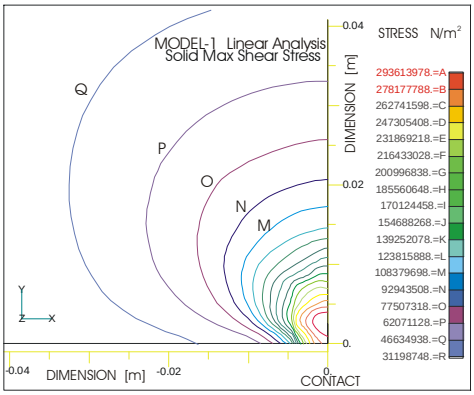

Fig. 5. Iso-lines for Tangent Stresses in the Linear Contact Analysis (MODEL-1)

Table T2

Band of parabola	1	2	3	4	5	6	7	8
Pressure p_i [N/m^2]	$1.1300 \cdot 10^9$	$1.0761 \cdot 10^9$	$0.9865 \cdot 10^9$	$0.8609 \cdot 10^9$	$0.6995 \cdot 10^9$	$0.5022 \cdot 10^9$	$0.2690 \cdot 10^9$	$0. \cdot 10^9$
Average pressure p_{SR-i} [N/m^2]	$1.1389 \cdot 10^9$	$1.1031 \cdot 10^9$	$1.0313 \cdot 10^9$	$0.9237 \cdot 10^9$	$0.7802 \cdot 10^9$	$0.6009 \cdot 10^9$	$0.3856 \cdot 10^9$	$0.1345 \cdot 10^9$

3. NONLINEAR CONTACT ANALYSIS

3.1. MODEL-2: Contact Analysis Using Gap-elements

Nonlinearities in the contact tasks are qualified with the material nonlinearities, geometry and boundary conditions. The material non-linearity is determined by the class of "metal" materials with nonlinear elasto-plastic characteristics of stress-deformation [6], shown in Fig. 7. The yield characteristics are defined as multi-linearized stress and deformations curve. In this way the possibility is created for plastic deformities to appear. The geometrical non-linearities are caused by the elastic contact surfaces profile deformations. These deformations are small, because with the material and shape choice we seek rigid geometries which provide rolling on kinematic elements (pairs). The boundary conditions non-linearity is provoked by the variability of the supporting points with the contact forces growth to the full value. The contact forces are the forces of working pressure and friction.

MODEL-2 is formed by taking into account the rigidity and boundary conditions changeability. This was performed using gap elements, with rigidity so tuned to correspond to the rolling body rigidity.

Gap elements are assigned the gaps of the contact surfaces based on outline geometry. The analysis treated the symmetrical half of the model. The whole model is presented in Fig. 6. The rigidity of **gap** elements is defined by average rigidity of middle rolling body support. With the group of **Gap** elements in the contact zone the changeability of gap between the curvature of the cylinder and the plate of rolling support was comprehended. The geometry and the **gap** dimensions are given in Fig. 6.

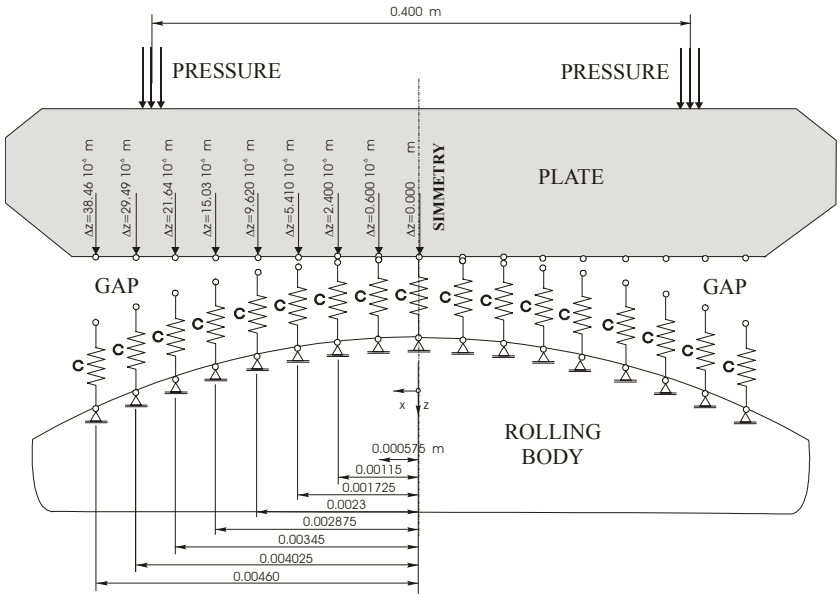

Fig. 6. MODEL-2: Modeling of the Supports in Non-linear Contact Analysis Using Gap Elements along the Contact Outline

According to the *Prandtl-Reuss* elasto-plastic problem generalization, the plastic deformations increment is proportional to stress deviator [3]. Appropriate to this model, the total stress state was determined according to the equivalent increment of plastic deformation and equivalent stress. The equivalent stress in plastic area σ_e corresponds to normal component stresses $\sigma_x,\sigma_y,\sigma_z$ and tangent stresses $\tau_{xy},\tau_{yz},\tau_{xz}$, and also is proportional to octahedral shear stress τ_{okt}[3], as shown in relation (5):

$$\sigma_e = \frac{1}{\sqrt{2}} \cdot [(\sigma_x - \sigma_y)^2 + (\sigma_y - \sigma_z)^2 + (\sigma_z - \sigma_x)^2 + 6 \cdot \tau_{xy}^2 + 6 \cdot \tau_{yz}^2 + 6 \cdot \tau_{xz}^2]^{0.5} = \frac{3}{\sqrt{2}} \cdot \tau_{okt} \quad (5)$$

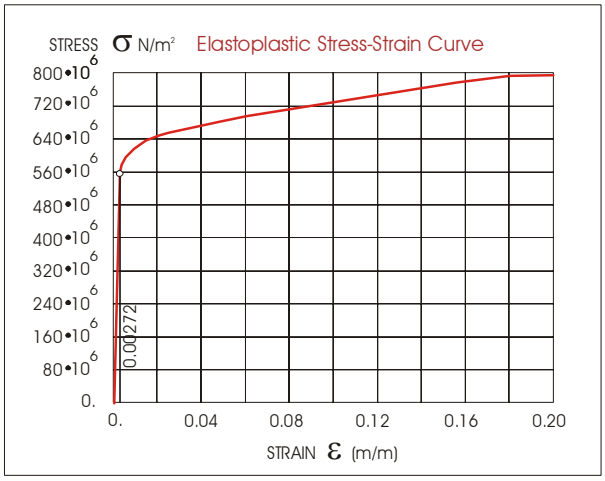

Fig. 7. Curve of Elasto-plastic Stress-strain Material (Chrome-nickel Steel)

The task was solved using the full incremental *Newton-Raphson* method. The displacements until reaching the contact are large. The procedure is based on iterative solutions of the equation:

$$[K_{n,i}^T] \cdot \{\Delta u_i\} = \{F_n^a\} - \{F_{n,i}^{nr}\} \quad (6)$$

In equation (6) $[K_{n,i}^T]$ is the Tangent rigidity matrix for step *n* in iteration *i* in *Newton-Raphson* method. $\{F_n^a\}$ is overall (absolute) force vector in the step n, while $\{F_{n,i}^{nr}\}$ is force vector for step *n* in iteration *i*. $\{\Delta u_i\}$ is the vector of the searched solutions for node displacements of the discrete system. *Newton-Raphson* large displacements method (T*he large strain analysis*) is always recommended when as the consequence of the contact bodies results in their shape change or change of the contact surfaces orientations. The iterative process convergence is achieved when residuum is less than the tolerance for the given value. Default tolerance value is 0.001. The convergence was checked using L2 norm (Euclid norm), which is formed as a square root of the sum of unbalanced forces, squares R_i , in all degrees of freedom given in equation (7). Using the same geometry as

[3] Octaedric shear stress depends on plasticity

in the previous linear model, the analysis with the results given in Figs. 13, 15 and 17 was performed.

$$\left\|\{R\}\right\|_2 = (\sum R_i^2)^{0.5} \quad (7)$$

3.2. MODEL-3: Contact Analysis Using Contact Pairs

The modern contact tasks analysis is carried out by means of the **method of direct constraints**. It is realized using contact pairs [6,7]. The contact pairs in the cylinder and surface contact are **contact surfaces**. Hereby the **target** and the **contact** surfaces are defined. The method follows the kinematics of the contact surface, resulting in boundary conditions defined in the moment of contact, along with further movement restriction. In the touching nodes contact forces F_i are applied. This method determines: the collective of finite elements where the bodies are in contact, the collectives of nodes that potentially can get in touch and the edges that potentially get in touch.

The given discrete 3D mesh passes through these contact boundary surfaces. The nodes in the contact area are the contact analysis carriers. To these nodes the spherical (pinball) tolerant potential contact areas are assigned, Fig 8.

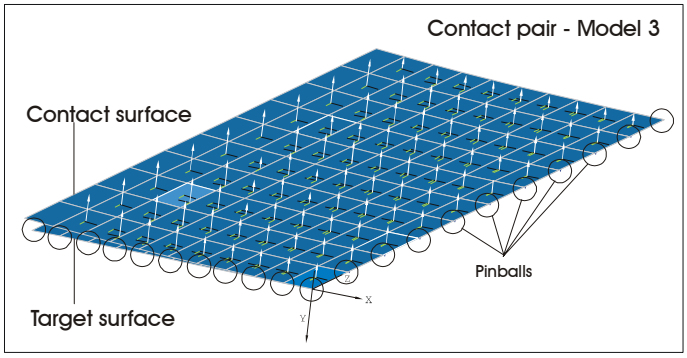

Fig. 8. Contact Model "Surface-to-surface"

When the node of other contact surface enters a tolerant array, the mechanical conditions of the contact are placed. The way of pressure realization, the movement direction, possible sliding, and the rigidity of target surface nodes are defined.

This is realized using the *Gauss* method. It identifies the Gaussian points that are in contact, as well as those which are out of contact and those near contact. In this way the non-linear analysis boundary conditions are defined, which do not depend on the initial assumptions about the contact pair rigidity. The rigidity of the real contact points is determined in details in every analysis step. In this way the assumptions about the model rigidity are eliminated and the real contact points' rigidity is used. The solution is obtained using the *Full Newton-Raphson method*. *The Penalty method* can also be used.

The ANSYS software uses contact the *Augmented Lagrange algorithm*. The concept of Gauss allows modeling of different mechanical models' contact situations. These are the situations of penetration, the preceding penetration, possibility/impossibility of separation and large/small contact deformations. In the tetrahedral or wedge elements applica-

tion, the contact surfaces are triangles and they do not have to obtain the full topological contact up to the element edges. As a result, the nonsymetry of the finite elements engaged appears in the contact pair. This possibility is given by the analysis algorithm, which improves the numerical stability. Also, in this kind of analysis the initial closing can be given – the dimension of the contact applied. This eliminates the situation in which the Gaussian points do not identify the whole contact area, or that they pass one through another without cutting in the two neighboring iterations.

The tribological phenomena of inner friction are implemented in the contact ask using exponential function (8), [6]:

$$\mu = \mu_d \cdot [1 + (k-1)^{-d \cdot v}] \tag{8}$$

In equation (8), $\boldsymbol{\mu}$ is the theoretical friction coefficient, $\boldsymbol{\mu_d}$ is the dynamic friction coefficient, **k** is the static and dynamic friction quotient, **d** is decay coefficient (sec/m), **v** is the slip rate (μ=0.2).

The given task of the MODEL-3 has 10150 3D solid basic elements, 100 contact elements **TARGE 170** and 100 contact elements **CONTA 174**. Taking into account the model symmetry, the problem was described with 12155 nodes and 34425 degrees of freedom[4]. Figs. 9, 10, 11 illustrate details of the non-linear contact analysis results for the whole MODEL-3 (shown in Fig. 1). The analysis comprises both the contact bodies.

Fig. 9 shows the array of the maximal normal component stresses[5], which amounts to $1160.\cdot 10^6$ N/m^2. Fig. 10 shows the array of maximal tangent component stresses for both the elements in connection. Fig. 11 shows the disposition of the model displacements. In this model, while the outer forces work on the plate ends, the displacements of the plate ends are the largest. The smallest displacements are in the middle of the cylinder, where the bodies contact is obtained.

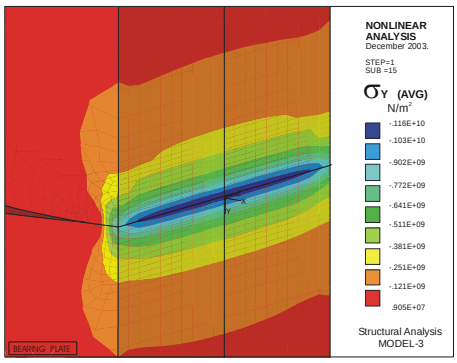

Fig. 9. Contact Zone Detail – Normal Component Stresses σ_Y (MODEL-3)

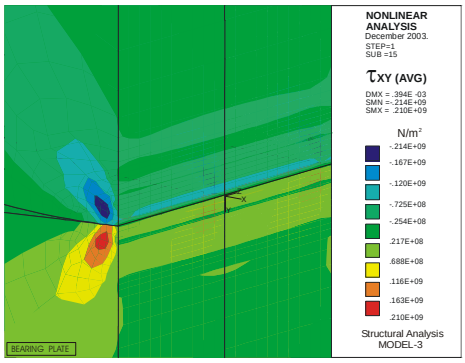

Fig. 10. Contact Zone Detail - Tangent Component Stresses τ_{XY} (MODEL-3)

[4] The realization on PC Intel P4/1.8 GHz was carried out in 960 sCP, with n=17 steps and average 100 subiterations.

[5] This value approximately corresponds to the surface pressure integrational constant in MODEL-1.

It is obvious that the modeling made in this way involves both the constructive elements, with the contact characteristics better described. Furthermore, the prosperous contact zone determination was carried out, based on its micro-deformation kinematics.

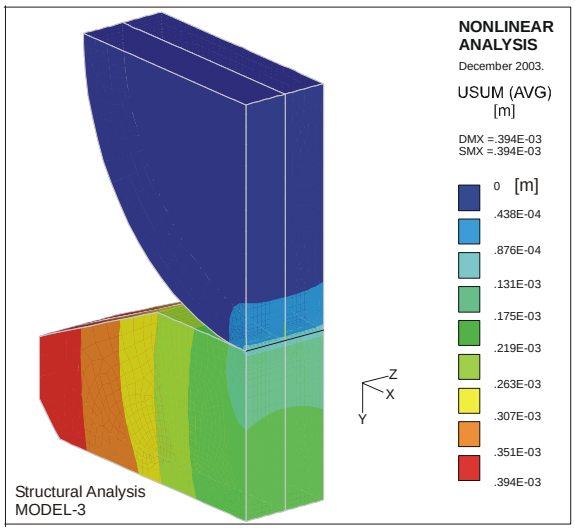

Fig. 11. Contact Analysis Using Contact Pair Result – Node Displacements (MODEL-3)

In this way the complexity of the contact geometry mechanism was improved. The friction characterized by the "steel-to-steel" model was involved, as used in friction joints. The use of the real material characteristics gives the realistic picture of stresses (Fig. 14), based on numerically determined deformations. It primarily refers to the situation of elasto-plastic deformation state, which is identified in this analysis and the damages on the real object found experimentally [5].

4. RESULTS ANALYSIS

The calculated results for the stresses and deformations give the basis for the contact pair accuracy evaluation. Deformations are a non-adequate evaluation criterion because the reliance conditions for the used models differ significantly. Therefore, the equivalent stresses calculated according to the theory of the biggest deformation work used for shape deformation (*Hencky-Humer-Mises*, better known as *Von Mises*) are the basic criteria for the engineering model validity evaluation. Principal stresses σ_1, σ_2, σ_3 are calculated as based on component stresses σ_x, σ_y , σ_z , τ_{xy} , τ_{yz} , τ_{xz} and maximal tangent τ_{MAX}. The following table T.3 gives an overview of all the three analyses. The compound stresses in the linear analysis have overcome equivalent ones from the non-linear analysis maximally by 5.42%. The smallest deviations are those among the non-linear analyses amounting to 3.05%.

In Figs. 12 and 13 the iso-surfaces for the linear and non-linear analysis of the middle part of the plate are compared (one cross section). These results do not contain the edge concentration stresses in the plate in the contact zone and at the end of contact. The ex-

treme values determined in this way are shown as mentioned bellow in Table T3. Fig. 14 shows the equivalent stresses for the MODEL-3. The stress distribution similarity is obvious. The largest compound stresses according to Figs. 12, 13, 14 show up in the linear analysis. They are negative effects of the linearized characteristics stress-deformation defined with the elasticity modulus E=const.

Table T.3. Model Analyses

	MODEL-1 Linear analysis	**MODEL-2** Nonlinear analysis - GAP	**MODEL-3** Nonlinear analysis CONTACT PAIR
Number of elements (3D)	11388	11388	10150
Number of **gap/contact** elements (1D)		270	200
Node number	12852	12960	12155
Degree of freedom (DOF)	37437	37050	34425
Max. **VonMises** stress in contact array (N/m^2)	595295008.		
Max. **Equivalent** stress in contact array (N/m^2)		580734976.	563340000.
Max. **Tangential** stress in contact array (N/m^2)	283323185.	320351542.	210000000**
Deformation (on force vector trace) Δy (m)	0.0001702	0.0000456*	0.000394
* Deformation – in contact array			
** Component of tangent stress			

In the linear analysis, larger deformations gave larger stresses, not the identification of plasticity. The calculated equivalent stresses in non-linear analyses MODEL-2/MODEL-3 are close ($580.735 \cdot 10^6$ / $563.000 \cdot 10^6$, N/m^2) and they are caused by the different contact rigidity. In MODEL-2 the average rigidity constant of GAP element was used. The calculated contact stresses are not only the consequence of the contact pressure, but also of the plate bending. In the analysis MODEL-3 the friction stresses of lower order showed up, Fig. 19. The equivalent plasticity stresses (in the contact zone) of MODEL-3 are given in Fig. 18.

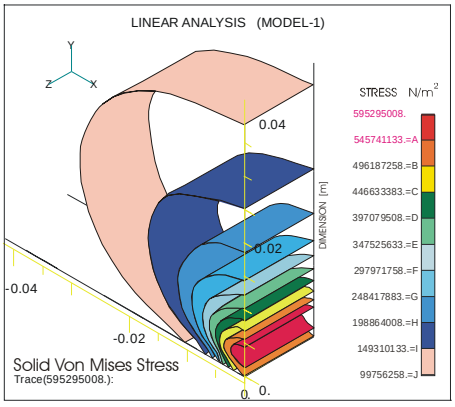

Fig. 12. Von-Mises Stresses Iso-surfaces in Linear Analyses (MODEL-1)

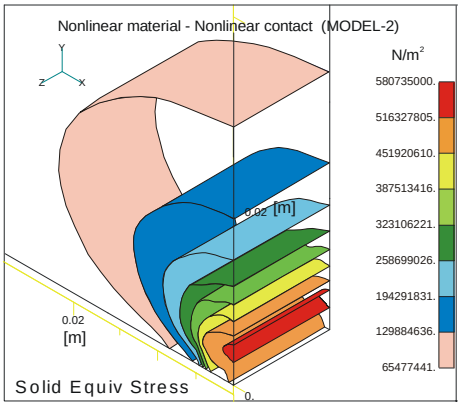

Fig. 13. Equivalent Stresses in Non-linear Analysis (MODEL-2)

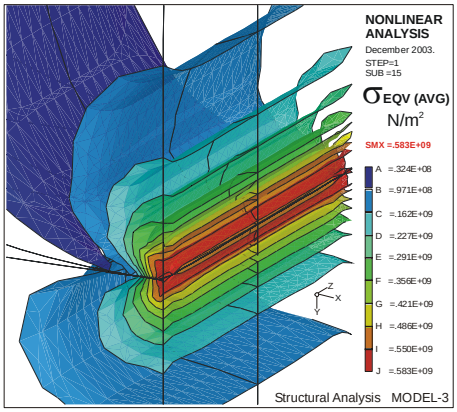

Fig. 14. Equivalent Stresses in Non-linear Analysis (MODEL-3)

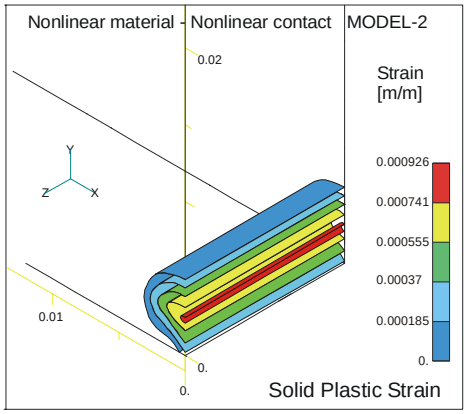

Fig. 15. Contact Zone – Solid Plastic Strain in Non-linear Contact Analysis (MODEL-2)

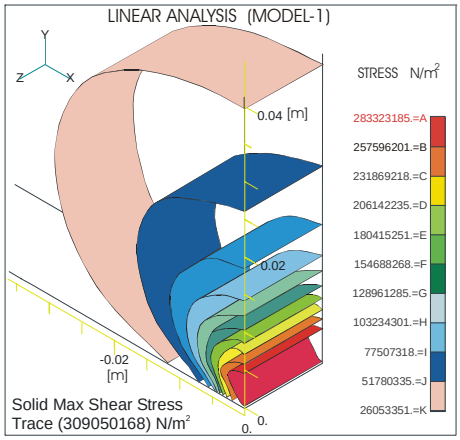

Fig. 16. Tangent Stresses Iso-surfaces in Linear Analyses (MODEL-1)

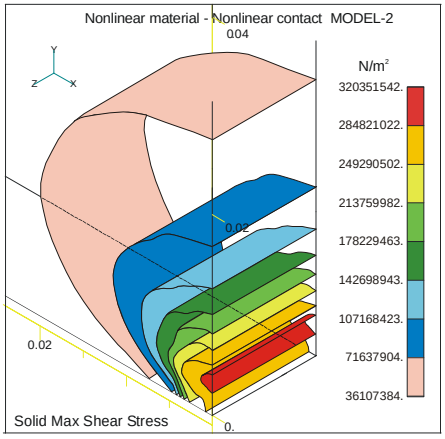

Fig. 17. Tangent Stresses Iso-surfaces in Non-linear Analyses (MODEL-2)

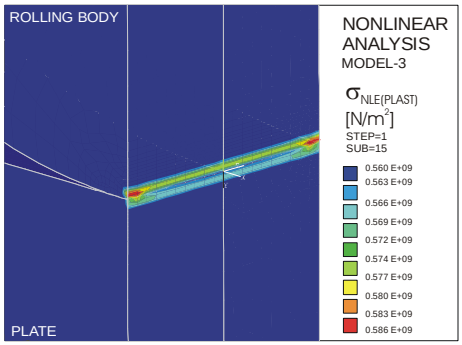

Fig. 18. Equivalent Plastic Stresses in (MODEL-3) (in the Contact Zone)

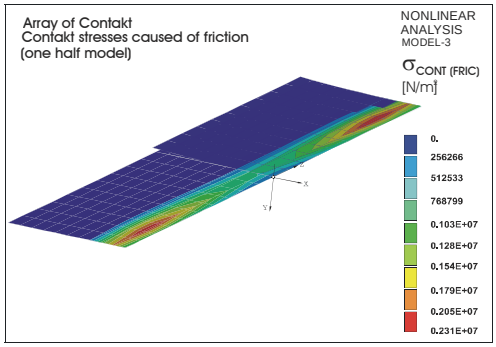

Fig. 19. Contact Friction Stresses in MODEL-3 (the Contact Zone)

5. CONCLUSION

The whole analysis is an example of the complex responsible structure treatment. The contact zone is the place of the highest stress in the support plate. The stresses obtained by this analysis represent the spatial state of stresses which comprises the plate deflection influence (as global deformation) and contact pressure (as local deformation). The classical *Hertz* theory and the existing regulations for constructions offer safety coefficients and allowed stresses for tensile, bending, shear and contact pressure cases, but not for a combination of influences of bending and surface pressures for the spatial state of stresses.

The obtained maximal stress $\sigma_{VON\ MISES}$=595295008. N/m^2 in the linear contact analysis is larger than contact stress in non-linear analyses as the consequence of plastic material deformation. The appearance of large stresses points out to the existence of plastic yield stresses and the risk which brings along the linear analysis. The compound stress is, on the other hand, much larger than the bending stresses, calculated by using the classical bending theory procedure (σ_S=125·10^6, N/m^2). The combination of contact influence and bending of the plate can only be viewed, for now, through equivalent stress. The comprehension for the shearing and normal stresses influence and the plastic states elimination is the necessary category for the definition of the contact element construction. This can be efficiently realized using the contact analyses group for the known geometry whose maximal structural action is searched for.

REFERENCES

1. Zienkiewicz O.C., Adaptivity and Mesh Generation, Int. Journal for Numerical Methods in Engineering Vol. 32, 783-810, 1991
2. Timoshenko S., Strength of Materials, Part II, Princeton, New Jersey, 1956
3. Kojić M.: Applied Theory Plasticity, University of Kragujevac, 1979
4. Sekulović M., Actual Problems of the Nonlinear Analysis, Architectural book, Belgrade, 1992
5. Jovanović M., Vacev T., Jovanović M.: Stress-Strain Sliding-Plate Support Analysis of the Middle Head, Naval Shiping Port the Power-Station "Đerdap-1" Kladovo, Report, Mininstitut, MIN Holding Co., Niš, 1998
6. ANSYS - Release 7.0, Theory Reference, Nonlinear Structural Analysis, 2000
7. MSC/NASTRAN for Windows V 4.0, Theory Reference, FEMAP, 1998
8. ALGOR-SSAP0H, V11.08-3H, Reference 1996

APROKSIMATIVNI KONTAKTNI MODELI KOTRLJAJUĆIH OSLONACA

Miomir Jovanović, Predrag Milić, Danko Mijajlović

Radom je posmatran kontaktni zadatak velikih kotrljajućih oslonaca koja se koriste na industrijskim i gradjevinskim objektima. Jedno od osnovnih pitanja je izbor analize za proveru nosivosti kontaktnih elemenata. U radu je uporedno primenjena linearna i nelinearna kontaktna statička analiza. Cilj je da se na bazi konkretnih primera utvrde aproksimacije i razlike u rezultatima. Najpre je izvedena linearna numerička analiza, metodom konačnih elemenata, zasnovana na klasičnom konceptu Hertz-a. Pri tome su uslovi oslanjanja nepromenljivi u toku delovanja opterećenja dok je sila aproksimovana površinskim pritiskom po zakonu parabole

drugog reda. Prikazan je jedan aproksimativan postupak odredjivanja površinskog opterećenja. Tako dobijena rešenja linearne analize su uporedjena sa analizama zasnovanim na nelinearnoj teoriji kontakta. Nelinearne analize bolje definišu distribuciju napona u strukturi jer koriste promenljivost graničnih uslova, uvode trenje, klizanje i krutost kontaktnih tela. Rad dalje pokazuje, modeliranje istog kontaktnog zadatka kroz dva različita nelinearna modela i poredjenje sva tri modela. Rezultati su izloženi grafički i numerički. Pokazane su mreže konačnih elemenata, osobine modela i složeni naponi u kontaktnim elementima. Objektivnu ocenu ovih analiza, dalo je ponašanje oslonaca u praksi.

Ključne reči: *Kontaktni par, FEM, kontaktna analiza, kontaktni modeli, aproksimativni modeli*